Numerical Simulation of the Meso-β Scale Structure and Evolution of the 1977 Johnstown Flood. Part III: Internal Gravity Waves and the Squall Line

DA-LIN ZHANG

National Center for Atmospheric Research, Boulder, Colorado*

J. MICHAEL FRITSCH

Department of Meteorology, The Pennsylvania State University, University Park, Pennsylvania

(Manuscript received 22 July 1987, in final form 30 September 1987)

ABSTRACT

The interaction between internal gravity waves and a squall line that developed early in the evolution of the 1977 Johnstown flood event is studied based on available surface observations and a three-dimensional model simulation of the flood-related mesoscale convective systems (MCSs). Several experimental simulations are carried out to investigate the mechanisms whereby gravity waves form and obtain energy. Both observations and model simulations of the wave/convection interaction fit certain theories of gravity wave propagation. Following the formation of the squall line, subsequent deep convection typically initiates behind a pressure trough associated with the line and ahead of or along the axis of the trailing ridge. The zero contours of vertical motion correspond closely to the axis of the surface pressure trough. Positive potential temperature perturbations correspond with descending motion occurring ahead of the trough while negative perturbations occur with increasing ascending motion towards the approaching ridge axis. Model airflow trajectories show that the simulated gravity wave surface pressure perturbations (with amplitudes of about 1 mb) correspond to vertical parcel displacements of more than 30 mb.

The model simulations indicate that the gravity waves are initiated by a super-geostrophic low-level jet with strong horizontal wind shear over an area where an explosive convective development occurs, and then are enhanced by intense convection. The waves propagate at a speed significantly faster than a meso-α scale quasi-geostrophic wave that is partly responsible for the initial explosive development and that later plays a key role in controlling the evolution of a mesoscale convective complex (MCC). The fast moving gravity waves help the squall line accelerate eastward and separate from a trailing area of convection that later develops into the MCC. It appears that the waves and the squall line interact with each other constructively prior to the squall line's mature stage. Specifically, the line of deep convection seems to provide the waves with energy through enhancing mass convergence/divergence in a deep layer and acting as an "obstacle" to the sheared flow. The waves tend to help organize convective elements into a line structure and turn the line a little clockwise. After the squall line moves into a convectively less favorable environment, it slows down, whereas the accompanying gravity waves continue their eastward movement. Then the convection and gravity waves gradually become out of phase and interact with each other destructively. Because of the absence of low-level inversions and critical levels to duct the wave propagation, the gravity waves quickly diminish as they move away from the energy source region. Free-wave experimental simulations show many wave characteristics similar to the control simulation, indicating that the gravity waves determine the orientation, propagation and structure of the squall line. A sea breeze circulation and mountain waves associated with the Appalachians also occur in the model simulation, but do not seem to have a significant effect on the evolution of the daytime deep convection.

The results indicate that physical interaction between deep convection and internal gravity waves can be simulated by numerical models if a compatible grid resolution, proper model physics and good initial conditions are incorporated. In particular, the apparent relationship between the gravity waves and the squall line suggests that preserving the components of layered internal gravity waves in the model initial conditions may be very important for successful model prediction of the timing and location of wave-related MCSs.

1. Introduction

Since Tepper (1950; 1955) inferred the presence of internal gravity waves (based on the fact that squall lines sometimes propagate significantly faster than the accompanying cold front), numerous observational studies have revealed the existence of large amplitude gravity waves associated with mesoscale convective systems (MCSs) (see the review paper by Uccellini and Koch, 1987). For example, using routine surface observations, Bosart and Cussens (1973), Eom (1975), Uccellini (1975), Bosart and Sanders (1986) and others noted gravity waves having amplitudes of 2 to 6 mb, periods of wave trough passage of 2 to 4 hours and

* The National Center for Atmospheric Research is funded by the National Science Foundation.

Corresponding author address: Dr. Da-Lin Zhang, NCAR, P.O. Box 3000, Boulder, CO 80307-3000.

propagation speeds of 20–50 m s^{-1}. A theoretical study by Einaudi and Lalas (1975) shows that pressure jumps associated with these waves are capable of generating upward motion strong enough to trigger convective storms when the atmosphere is close to saturation. In fact, Mastrantonia et al. (1976) and Stobie et al. (1983) have presented evidence of the reorganization of preexisting convective activity and new development of more cloud clusters downstream of the wave origin. Furthermore, Miller and Sanders (1980) found that the preexisting convection was considerably enhanced at the time of the wave passage. Thus, it appears from the literature that internal gravity waves are one of many important mechanisms whereby MCSs develop, propagate and produce significant rainfall.

There are a number of physical processes responsible for the generation of gravity waves. These include vertical shear instability (see Mastrantonio et al., 1976; Gedzelman and Rilling, 1978; Bosart and Sanders, 1986), intense convection or wave-CISK (see Curry and Murty, 1974; Balachandran, 1980; Lindzen, 1974; Raymond, 1976; Raymond, 1983), horizontal nonuniform flow (see Einaudi, 1984), pressure jump at the interface between fluids of different densities (see Tepper, 1950; 1955), and topographical forcing (see Gossard and Hooke, 1975; Atkinson, 1981). Using a two-dimensional cloud model, Clark et al. (1986) found that gravity waves can be excited by thermal forcing, boundary eddies, and convective clouds acting as obstacles to the sheared flow, and noted that the wind shear (or the obstacle) effect is a more efficient generator of gravity waves than the pure thermal forcing. Christie et al. (1978) and Doviak and Ge (1984) showed that thunderstorm-generated pools of moist downdraft air can produce internal gravity waves that propagate faster than the downdraft outflow. In order for these waves to propagate for a long distance without changes in their properties, theoretical studies show that they require the existence of a low-level inversion bounded above by a layer of minimum stability that can reflect vertically propagating energy, and a critical level within the layer (see Lindzen and Tung, 1976; Lalas and Einaudi, 1976). Otherwise, the internal gravity waves would gradually dissipate after they propagate away from the energy source region.

One distinctive and essential feature of gravity wave propagation is that the wave-induced upward motion takes place in concert with rising pressure (Gossard and Hooke, 1975). Specifically, Eom (1975) and Uccellini (1975) showed that for a positive propagating wave (w.r.t. wind direction), the maximum rate of ascent in the lower troposphere should occur midway between the pressure trough and advancing ridge with maximum parcel displacement occurring at the pressure ridge.

It has been found that internal gravity waves also occurred in association with the MCSs (a squall line and a mesoscale convective complex or MCC) that developed during the 19–20 July 1977 Johnstown, Pennsylvania flood events (Zhang and Fritsch, 1986a). Both observations and the model simulation show a correlation between surface pressure perturbations and the occurrence of deep convection, particularly with the squall line (see Hoxit et al., 1978; Zhang and Fritsch, 1986a). The objective of this paper is to document the meso-β scale structure and evolution of the internal gravity waves and establish their relationship to the deep convection. In particular, the present study emphasizes the description of the numerical simulation (rather than observations) of the gravity wave interaction with deep convection since up to now, there is little documentation in the literature showing an apparent relationship between gravity waves and convective storms from the numerical modeling standpoint. In section 2, the observational evidence of the gravity wave propagation associated with the Johnstown MCSs is presented. Section 3 describes the model-simulated structure and evolution of the waves and their relationship to the MCSs. Wave origin and wave/convection interaction mechanisms are explored in section 4. Summary and concluding remarks are given in the last section.

2. Observational evidence

During the four-day period prior to the Johnstown flood, a succession of convective outbreaks occurred over the upper Mississippi Valley as a weak upper-level meso-α scale disturbance propagated from the Dakotas through the Great Lakes region toward Pennsylvania. These convective outbreaks apparently were responsible for the development of a supergeostrophic low-level jet over the Great Lakes region (see Bosart and Sanders, 1981). On the morning before the Johnstown flood (i.e., at about 1200 UTC 19 July 1977), the core of the low-level jet was approaching Lake Erie and an explosive development of convection ensued (see Figs. 1a and 1b). At this time, the axis of the meso-α scale trough had just reached Lake Erie, and a low-level wind speed maximum of nearly 19 m s^{-1} was located over eastern Michigan (see Fig. 2). Conditionally unstable lapse rates were observed from Michigan eastward into New York and Pennsylvania (e.g., see the soundings at Flint, Michigan and Pittsburgh, Pennsylvania in Fig. 3). Hoxit et al. (1978), Bosart and Sanders (1981), and Zhang and Fritsch (1986a) provide more detailed descriptions of the mesoscale prestorm environment and subsequent evolution of weather events.

As will be shown in the following two sections, the low-level jet over the Great Lakes appears to be responsible for the initiation of internal gravity waves through geostrophic adjustment processes. The waves tend to alternately accelerate and decelerate low-level flow and generate mass convergence and divergence, thus helping organize deep convection into a line

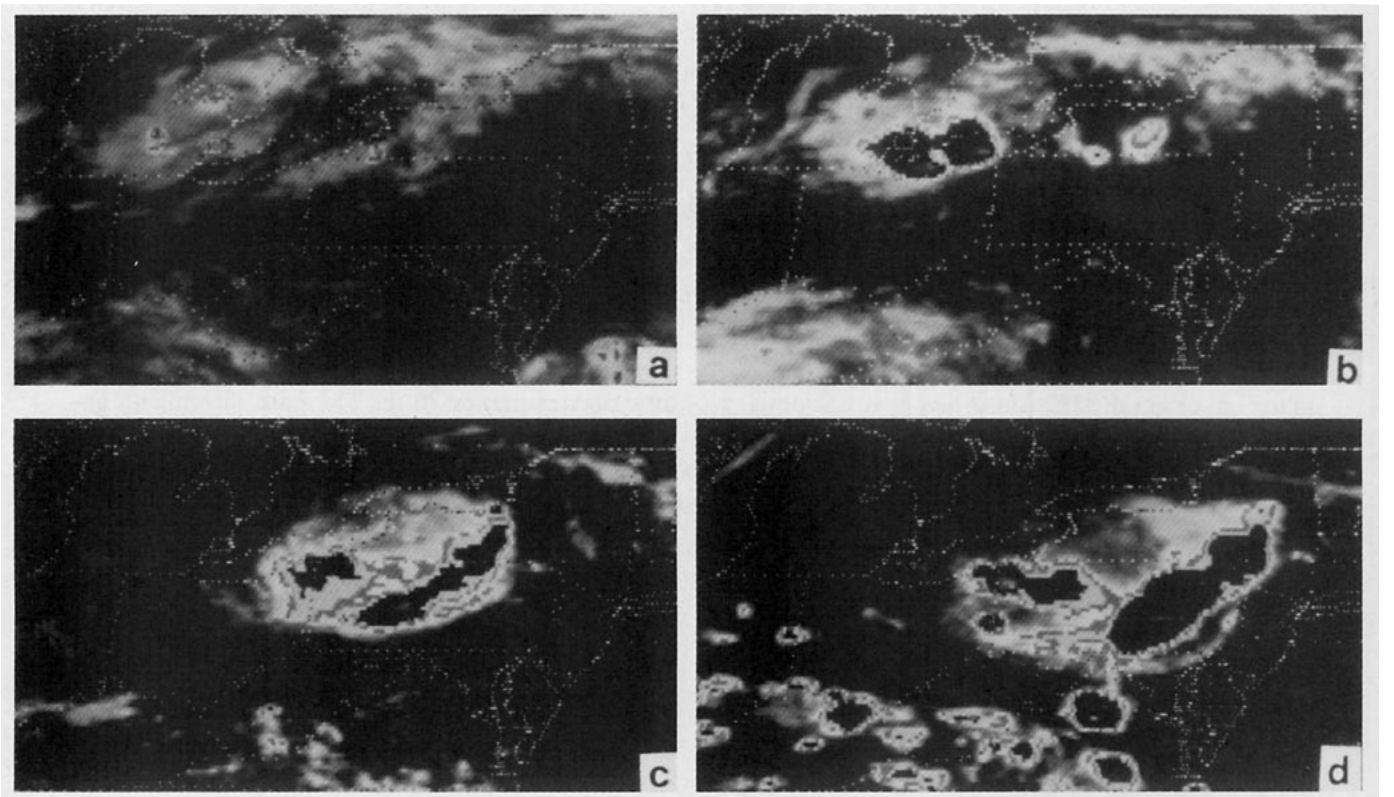

FIG. 1. Enhanced infrared satellite images for (a) 0900 UTC, (b) 1200 UTC, (c) 1800 UTC and (d) 2100 UTC, 19 July 1977.

structure. As the deep convection formed over Lake Erie, it quickly assumed a line-type structure and propagated east-southeastward across Pennsylvania (see Hoxit et al., 1978; Zhang and Fritsch, 1986a, and Figs. 1a–d). The gravity waves do not become clearly apparent from available surface pressure analyses until 1500–1800 UTC when both the waves and the squall line accelerate eastward and gradually separate from the initial area of deep convection. The acceleration of the wave–convection system as the surface pressure perturbation increases, qualitatively appears to obey the impedence relationship (Gossard and Hook, 1975). Based on the radar echo analyses by Hoxit et al. (1978), the squall line is in its strongest stage around 1800–1900 UTC. After that period, the squall line tends to dissipate. As the line moves across Pennsylvania during 1500–2100 UTC, deep convection typically initiates behind the pressure trough and ahead of or along the axis of the trailing ridge (see Hoxit et al. 1978; and Figs. 13 and 14 in Zhang and Fritsch, 1986a). In order to explore the possibility of a relationship between internal gravity waves and deep convection, the 4 day/page barograph traces encompassing the 24 h period when the MCSs traversed Pennsylvania are digitized, and the mean and diurnal trends are removed (see Fig. 4a). Note that the limits of accuracy for these digitized traces are 15–20 minutes in time and 0.1–0.3 mb in magnitude. Such accuracy appears to be satisfactory for identifying the apparent gravity waves in the present study of wave–convection interaction.

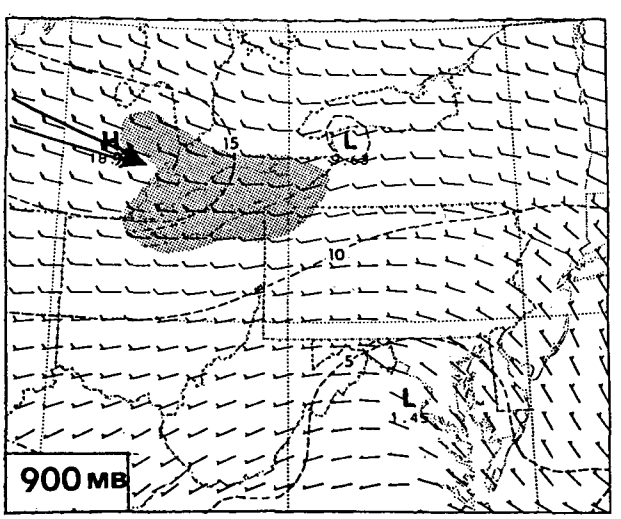

FIG. 2. Analysis of mesoscale wind speed (m s^{-1}) at 900 mb for 1200 UTC 19 July 1977. Large arrow indicates axis of maximum wind speed. Shading denotes the area of model-generated active convection.

In general, the traces at all sites indicate a slow early morning fall and an absence of wave activity prior to the convective events (see Fig. 4a). The waves start

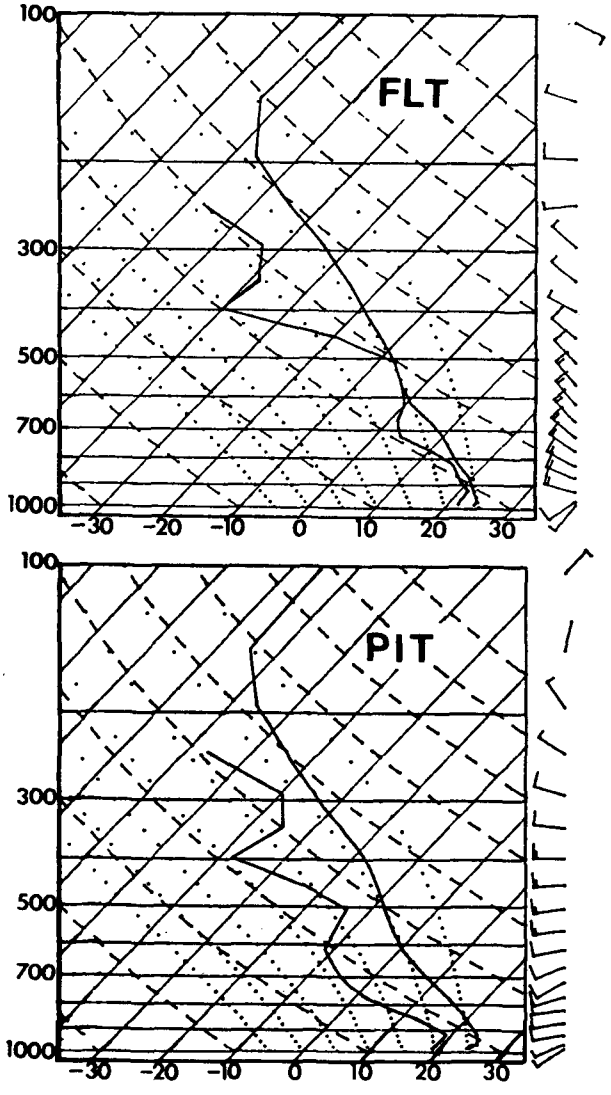

FIG. 3. Observed Flint (FLT), Michigan and Pittsburgh (PIT), Pennsylvania soundings at 1200 UTC 19 July (see points FLT and PIT in Fig. 4b). A full barb is 10 m s^{-1}.

with relatively small pressure rises and falls over 2–4 h periods, and are followed by a sharp pressure increase ("pressure jump"). The pressure jump corresponds to the arrival of cold outflow (i.e., a gust front) associated with the squall line. Note that there is an increasing period of slow pressure rise immediately prior to the arrival of the gust front (see the traces for IPT, AVP and ABE). Slow pressure rises ahead of the gust front were also observed by Goff (1976). One possible interpretation of this sequence of events is that the increasing period of slow pressure rise indicates a passing gravity wave propagating faster than the gust front. Another possibility is that a gravity wave was produced by the convection/gust front and is accelerating ahead of it. As the squall line/gravity wave advances eastward, its amplitude decreased while the amplitude of a trailing convective line/gravity wave increased. Note also that in the ABE trace, a slow pressure rise appears to be developing ahead of the trailing surge as well. These characteristics suggest that if gravity waves were present, they propagated faster than the cold outflow material. The faster propagation rate of the "gravity wave" can also be seen from the hourly positions of the gust front and the gravity wave front (start of the slow pressure rise). Based upon the Hoxit et al. (1978) mesoanalysis and available barograph traces, it is apparent in Fig. 4b that the wave front is moving faster than the gust front (25–30 m s^{-1} for the wave front vs 15–20 m s^{-1} for the gust front). Note that as the gravity wave propagated progressively farther ahead of the gust front, the gust front and associated squall line weakened and then rapidly dissipated after 2100 UTC (see Hoxit et al., 1978; or Zhang and Fritsch, 1986a). This suggests that the wave may have advanced far enough ahead of the squall line/gust front so that its vertical circulation interacted destructively with the generation of new convection.

The situation described above is similar to the case studied by Doviak and Ge (1984). Note though that such a scenario is not evident prior to 1800 UTC. It is therefore hypothesized that the waves and squall line may have evolved simultaneously, i.e., accelerated eastward and intensified in a "locked phase" relationship before their "mature stage" from around 1800–2200 UTC. Einaudi et al. (1987) presented another example of the locked phase relationship between deep convection and gravity waves. During the development period, the gravity waves are just disturbances superimposed in phase on the gust-related pressure jump and it is difficult to separate their individual components. It is important to point out that in the Johnstown MCSs case, the eastward acceleration and intensification of the waves and squall line are probably part of the reason why the squall line separated from the initial area of convection (see Zhang and Fritsch, 1986a). Specifically, following the initiation of the gravity waves and the explosive development of the MCS over Lake Erie at 1200 UTC, the waves propagated ahead of the MCS with a speed significantly faster than the forcing from the meso-α scale quasi-geostrophic short wave that helped initiate and organize the MCS (Zhang and Fritsch, 1986a). Thus, the waves and the induced leading line of the MCS could advance away from the initial convective region (pre-MCC) and separate from the geostrophic-wave-associated convection that continued over western Pennsylvania. This will be examined in the next section by computing model air trajectories relative to the wave propagation. Zhang and Fritsch (1987) found that the development of a mesovortex behind the squall line tended to help but not cause separation of the squall line from the pre-MCC.

3. Numerical simulation

The lack of high-resolution observations makes model simulations a potentially useful tool to study

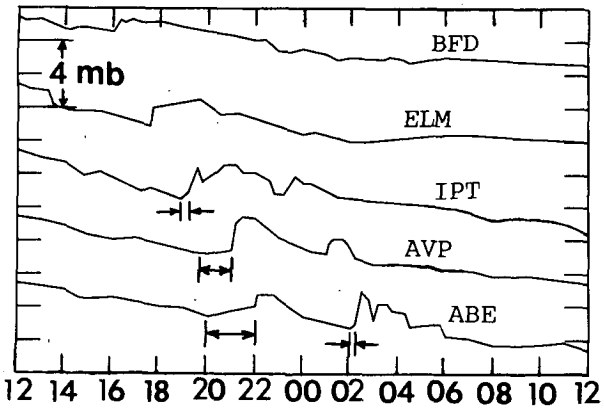

FIG. 4a. Digitized surface pressure traces at selected stations (see Fig. 4b) for 1200 UTC 19–1200 UTC 20 July 1977.

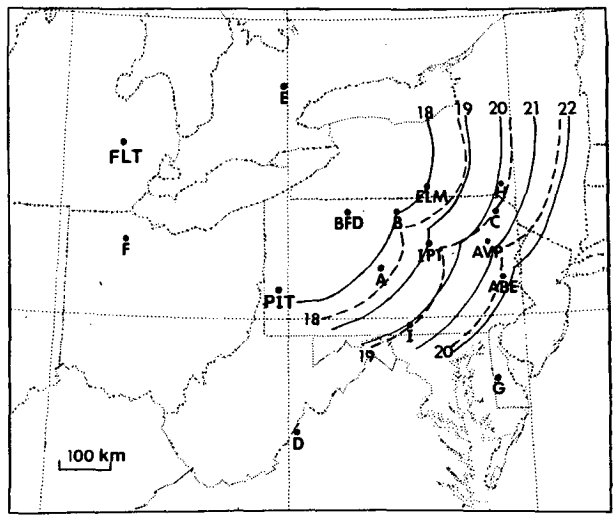

FIG. 4b. Hourly (UTC) position of the outflow boundary (solid lines) associated with the squall line (based on the analysis by Hoxit et al., 1978), and the analyzed wave front (dashed lines). Large dots indicate locations of surface stations (standard three-letter code) and model grid points (single letters).

the relationships between internal gravity waves and intense convection. As shown in Zhang and Fritsch (1986a), the model simulates fairly well the structure and evolution of convective events, associated surface pressure perturbations, and the planetary boundary layer (PBL). In particular, the observed eastward acceleration and separation of the squall line from the pre-MCC area of convection are well reproduced. In agreement with the observational analyses, the simulated squall line also becomes mature around 1800 UTC. Figure 5 shows the 1800 to 2100 UTC portion of the model-simulation of the squall line and pre-MCC. Although the basic configurations of the surface features conform reasonably well to the hourly observational analysis of Hoxit et al. (1978), the northern portion of the model convection propagates a little too quickly while the southern end moves too slowly. Furthermore, the simulated squall line appears to extend too far to the south (see Zhang and Fritsch, 1986a, for the verification). Nevertheless, the general agreement between the simulation and the observations is deemed adequate for using the model results to investigate the relationships between gravity waves and deep convection.

In order to show the model's capability in reproducing the observed wave activity, an approach similar to the preceding observational analysis is employed. Figure 6 presents the model-simulated surface pressure traces at a few selected grid points (see Fig. 4b for their locations). The time evolution of the fine-mesh domain-averaged trend has been removed from the pressure values for individual grid-point traces. The domain-averaged trace presumably represents the larger-scale variation of surface pressure, and is used here to separate pressure changes associated with the gravity waves from changes from larger-scale processes. The larger-scale pressure variation shows a slight rise during the first two model adjustment hours, and then a gradual fall for the remainder of the 12 h period (daytime). An oscillation with a period of about 2 h is evident; this may be a normal mode for the particular domain and governing system used for this study. Although at individual grid points there are some high frequency oscillations associated with external gravity waves, they are not as significant as that described in Anthes et al. (1981) and Brill et al. (1985). The absence of large amplitude oscillations may be due to the use of a nested-grid technique, or the particular initialization procedure and dataset for this case study (see Zhang et al., 1986; Zhang and Fritsch, 1986a).

Comparison of the model-predicted evolution of the surface pressure field to the observed evolution reveals a scenario similar to the observed. For example, after some initial adjustments in the first two hours, the grid-point traces at A and B display a steady pressure fall as the model squall line approaches. This is followed by a sharp rise when the squall line arrives, and then a return to the background trends in about 1–2 h (see Fig. 6). Note that the high-frequency oscillations due to the fast moving external gravity waves are relatively insignificant when compared with the strong signals of the internal gravity waves. Specifically, the high-frequency oscillations have a period of about 1 h and an average amplitude of 0.2 to 0.3 mb while the meteorologically meaningful waves have a period of more than 5 h and an amplitude of about 1 mb. At other grid points far away from the MCSs, the magnitude of internal gravity waves is noticeably less and is contaminated by the external gravity waves (e.g., D–G in Fig. 6). The similar phases of the pressure traces at points A and B are due to the similar relative locations taken with respect to the orientation of the simulated squall

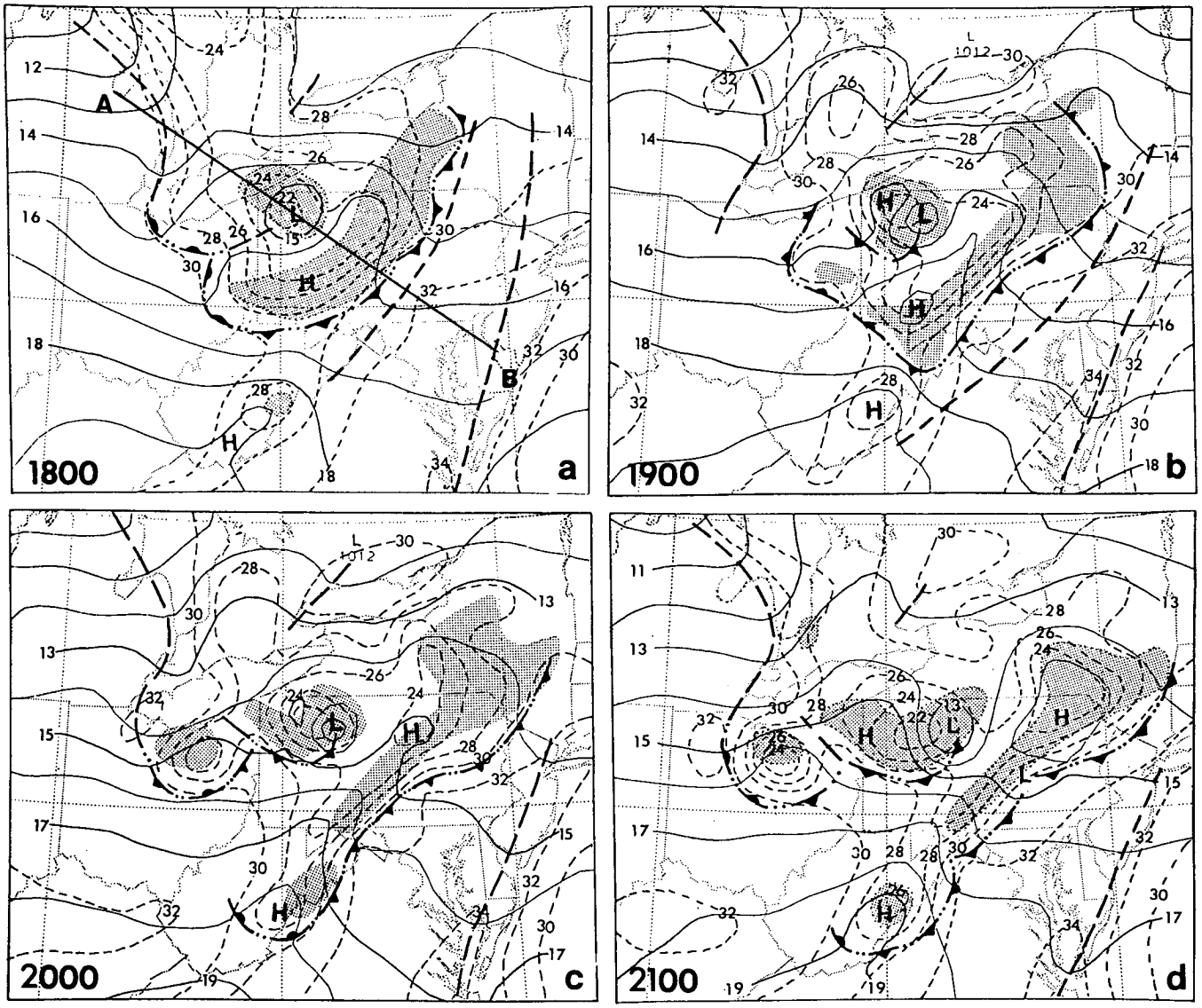

FIG. 5. Analysis of simulated sea-level pressure (solid lines, mb), surface temperature (dashed lines, °C), outflow boundaries (represented by frontal symbols), and troughs (heavy dashed lines) verified at the times as indicated. Shading indicates areas of active convection.

line (cf. Figs. 4b and 5a). Examination of the wave propagation from point B to C reveals that the wave tends to disperse as it propagates eastward. This same tendency is also evident in the observed traces (see Fig. 4a and compare the traces of the first wave as it moves through IPT, AVP and ABE). The duration of the pressure trough increases and the pressure jump gets progressively weaker as both the observed and simulated squall lines move eastward and gradually dissipate.

Figure 7 shows the predicted hourly surface pressure tendencies between 1800 and 2100 UTC over the fine-mesh domain. These pressure tendencies are the differences between values at the indicated time and 1 h before. Note that no smoothing was applied when generating the figure. There are several interesting features to be noticed here. First, there is an outward propagation of pressure tendency waves associated with the evolution of the model convection. At 1800 UTC, the shape and orientation of the first wave corresponds well to the position of the model squall line. Later on, the pressure tendency trough and ridge tend to propagate ahead of the model squall line and cold outflow material. At 2100 UTC, the first wave front moves almost out of the model domain. Although it is difficult to identify such wave structure from stations far away from the MCSs based on the available 4-day/page barograph traces, the simulated wave propagation ra-

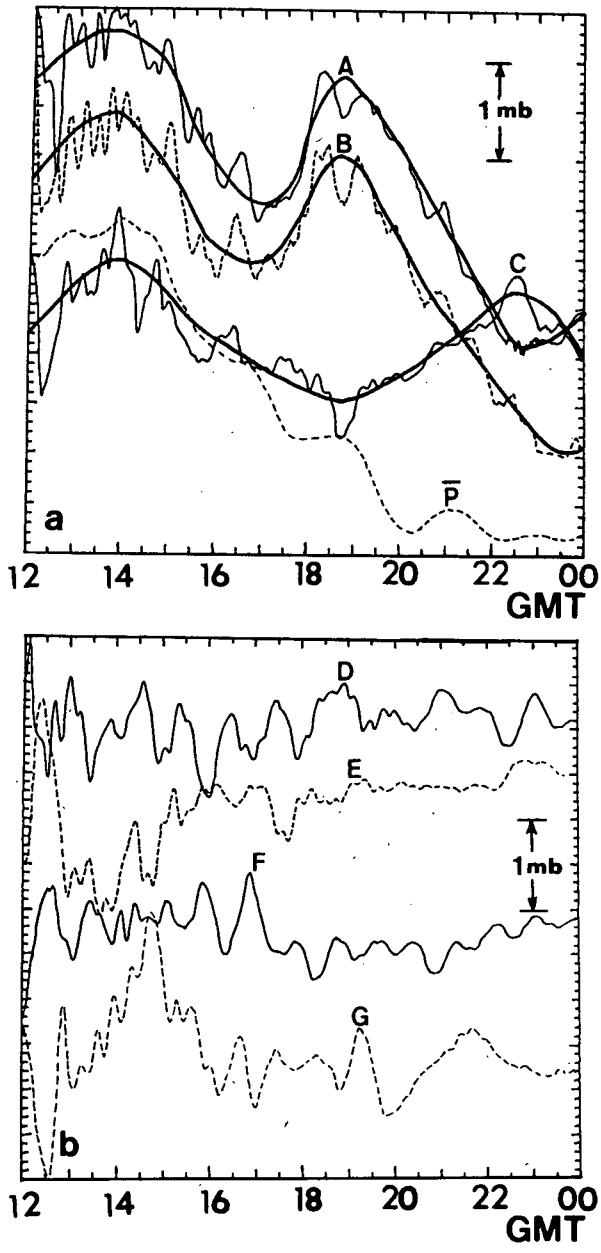

FIG. 6. Simulated temporal variation of surface pressure at 7 points (A to G, as located in Fig. 4b) and the fine-mesh domain-averaged surface pressure changes ($\bar{P}$). The thick solid lines are the subjectively smoothed surface pressure trend.

dially into more distant and extensive areas is to some degree consistent with wave propagation theory (see Gossard and Hooke, 1975). The simulated waves in the present case propagate with a speed of 25–30 m s^{-1} and a wavelength of 250–300 km. These values appear to be a little larger than what can be determined from the observations. This wavelength discrepancy is possibly due to the horizontal grid resolution of 25 km which may be too coarse to be utilized for simulating the present wave activity.

Second, note that from roughly central Pennsylvania northward, the model squall line remains in a favorable phase with respect to the gravity wave pressure tendencies, while the part of the squall line over southern Pennsylvania does not. Specifically, as the model squall line moves toward southeastern Pennsylvania and enters an unfavorable environment for generating new convection, the propagation rate of convection slows down (see Fig. 5) while the gravity wave continues its outward propagation with little change in speed. Around 2000 UTC, a pressure tendency ridge instead of a trough is located ahead of the squall line in south central Pennsylvania (cf. Figs. 5c and 7c). According to the Eom-Uccellini gravity wave theory, the passage of the pressure tendency ridge axis indicates a switch from forcing to suppression of the development of deep convection, as will be shown from air trajectory analyses. This corresponds to the dissipation of the observed and control-simulated squall lines. Correspondingly, there was no convection triggered as the pressure tendency perturbations advanced into the southeastern corner of the model domain.

Third, there is a large isallobaric pressure fall–rise couplet associated with a warm-core mesovortex that develops over northwestern Pennsylvania (see Zhang and Fritsch, 1987, for documentation of the vortex). This couplet does not seem to have much effect on the evolution of the first wave since a similar scenario for the first wave occurs in experimental simulations (see Zhang and Fritsch, 1988) in which the model fails to reproduce the mesovortex. (This point will be discussed further in the next section.) However, the isallobaric couplet appears to affect the evolution of events at a later stage. In particular, it contributes to the production of the second pressure wave (see Fig. 4a). Although the first wave is unable to trigger any convection as it propagates westward, the second wave generates a significant area of deep convection over northern Ohio around 2000 UTC (see Figs. 5c and 5d). In this situation, the model convection takes place in a reverse configuration with respect to the pressure ridge–trough system that occurred with the squall line. The phase relationship between the convection and the waves also fits the Eom-Uccellini gravity wave theory when a negative phase speed relative to mean wind is considered. A similar scenario of convective development was documented in the observations (see Hoxit et al. 1978). Both observed and control-simulated convective systems passed by the Pittsburgh area and eventually merged with the major MCC to produce the Johnstown flood episode.

Figure 8 displays the horizontal distribution of the model-simulated 850 mb vertical motion at times corresponding to that in Figs. 5 and 7. Although the distribution of significant upward motion is basically as-

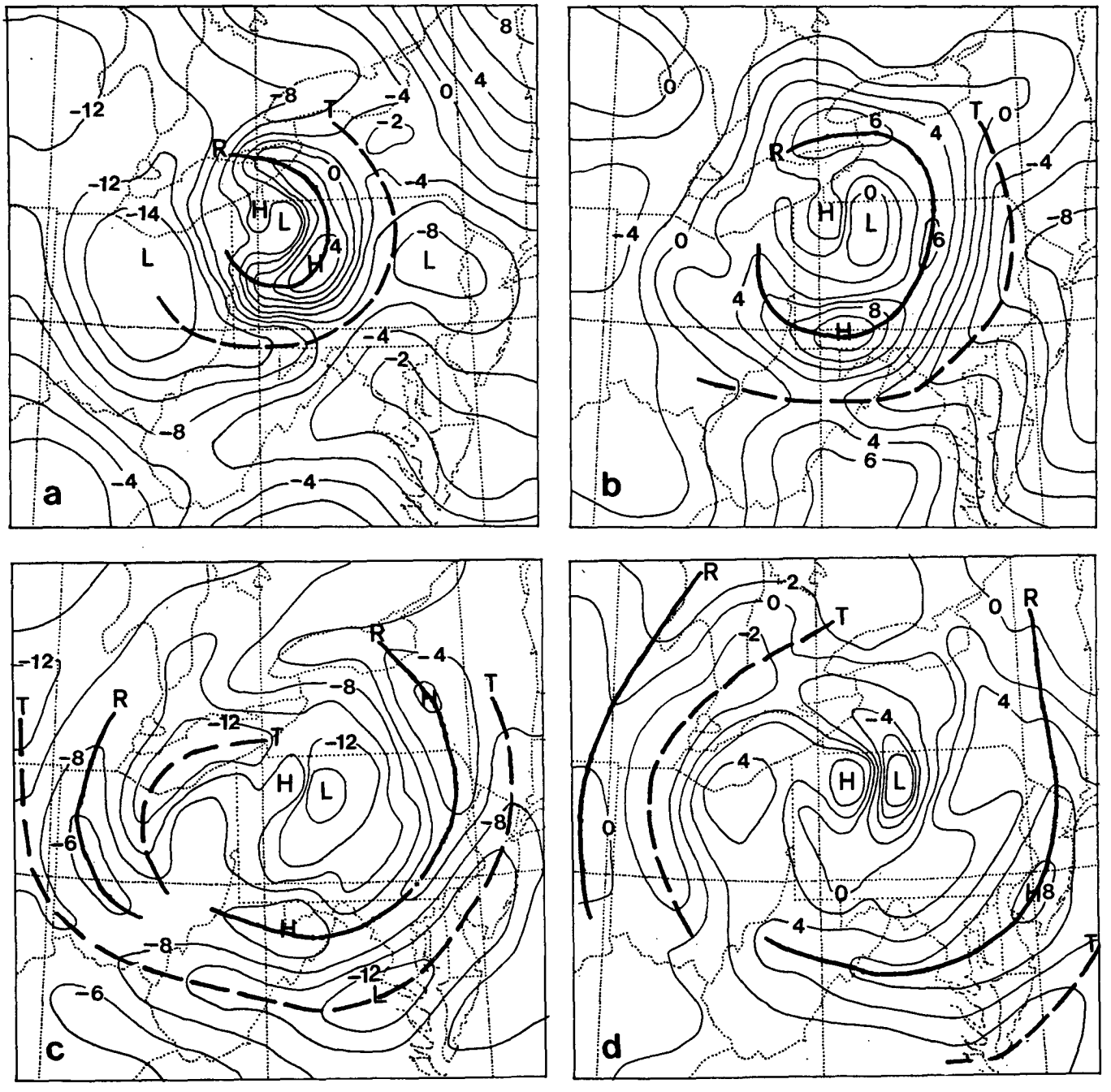

FIG. 7. Simulated hourly surface pressure tendencies (10^{-1} mb h^{-1}) at (a) 1800 UTC, (b) 1900 UTC, (c) 2000 UTC, and (d) 2100 UTC. "T" denotes the axis of a pressure tendency trough and "R" the axis of a pressure tendency ridge.

sociated with the forcing from the MCSs, the propagation of up/down wave motion is clearly apparent. In particular, a band of descending motion ahead of the simulated squall line propagates outward from the source region at a speed faster than the convective system. The propagation of this band corresponds to the pressure tendency trough of the first wave shown in Fig. 7 if the time difference used to compute the surface pressure tendencies is taken into account. The position of the surface pressure trough in the simulation roughly corresponds to the zero line of vertical motion, where sinking has occurred the longest, and thus where the lowest pressure would be expected. Hence, the subsidence warming by the propagating gravity wave is responsible for the generation of the pressure trough ahead of the squall line.

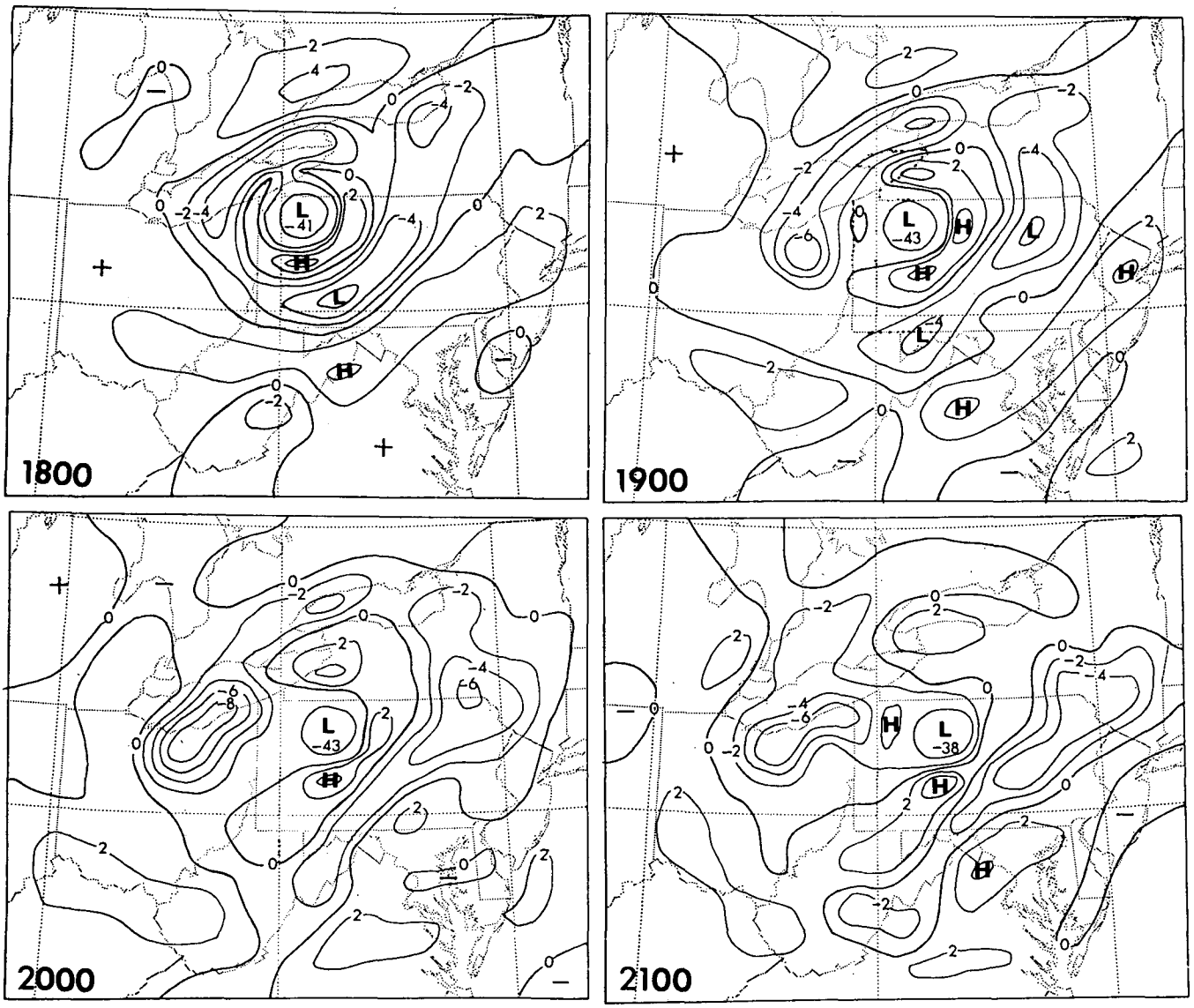

FIG. 8. Simulated 850 mb vertical motion (ω, μb s^{-1}) at (a) 1800 UTC, (b) 1900 UTC, (c) 2000 UTC, and (d) 2100 UTC.

As the first wave moves away from the squall line, the vertical motion pattern over southeastern Pennsylvania, Maryland and Delaware becomes less organized. On the other hand, the vertical motion with the northern portion of the squall line remains well organized and the line propagates at a speed faster than its southern portion but a little less than the gravity wave speed. This agrees with observations in which the northern part of the squall line is relatively longer lived and eventually dissipates over eastern New York.

To show why the northern and southern portions of the squall line behave differently, Fig. 9 shows two model soundings from similar relative locations with respect to and ahead of the convective system at 1800 UTC (see points H and I in Fig. 4b). Both soundings indicate a well developed mixed-layer up to 850 mb. However, the northern sounding exhibits a conditionally unstable stratification that requires only slight lifting for convection to take place whereas the southern sounding would require considerably more lifting to initiate convective overturning. Furthermore, the low-level horizontal anticyclonic wind shear with high values to the north would also tend to turn the wave trough axis clockwise (see Fig. 2) so that the southern portion of the wave moves relatively slowly.

The vertical structure of the internal gravity waves can be seen from a NW–SE vertical cross section of potential temperature (θ) and vertical motion (ω) (see Fig. 10). The gravity wave propagation is clearly evident through very deep layers of the atmosphere. Note that except for the active convection region, the amplitude of the wave-induced disturbances decreases with height.

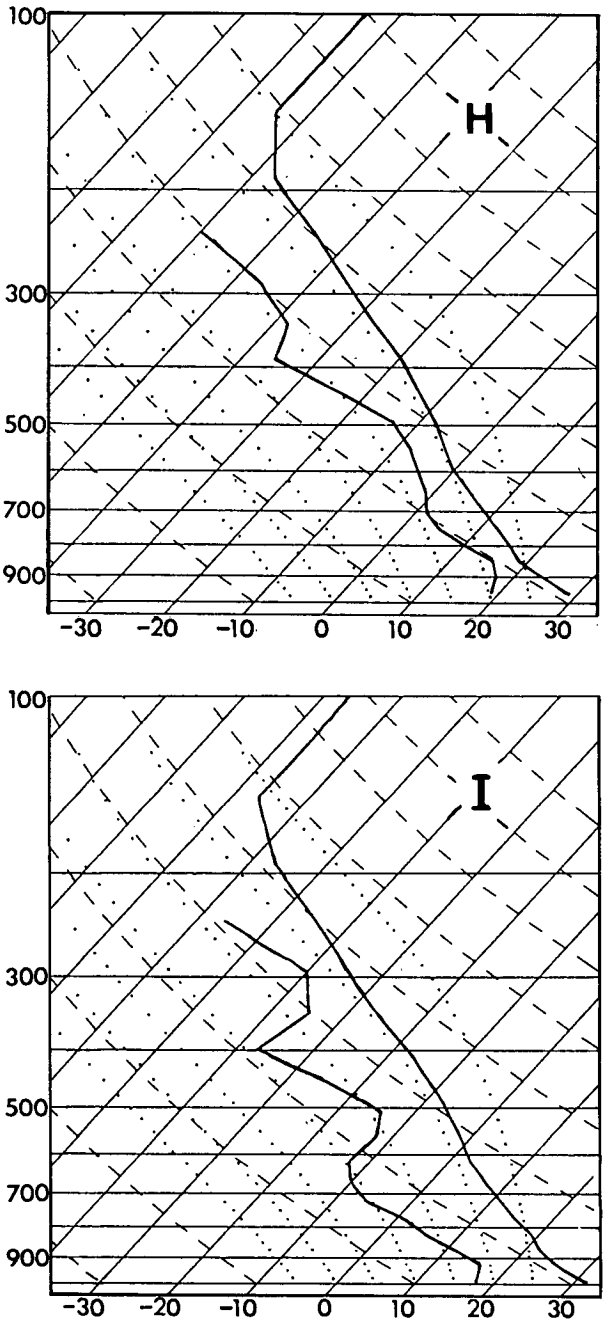

FIG. 9. Model-simulated soundings ahead of the squall line (see points H and I in Fig. 4b) from 6 h forecast verified at 1800 UTC.

Such vertically in-phase structure of waves may be a characteristic mode associated with penetrative deep convection. It appears that the mid- to upper-level convective and resolvable-scale heating and cool downdraft air play an important role in enhancing the wave activity. Specifically, the downdraft air with θ jump at lower levels behaves like a cold front or density current pushing the boundary layer air forward and upward. In a model run in which stronger moist downdrafts are produced by artificially changing precipitation efficiency in the Fritsch and Chappell (1980) cumulus parameterization scheme, model convection propagates outward in almost all directions (not shown). The resulting surface pressure perturbations are much stronger and propagate much faster than that in the control simulation. This experiment further supports the notion that moist downdrafts tend to enhance the wave forcing through generating strong pressure gradients and blocking the lower-level flow. On the other hand, the convective heating tends to induce lower- to midlevel convergence and surrounding compensating divergence, thus further helping enhance the wave motion. It appears that the midlevel heating is more effective in enhancing the wave amplitude than moist downdrafts, as also pointed out by Raymond (1984). In fact, Zhang and Fritsch (1988) have shown that without the convective heating, the simulated squall line is poorly organized and the moist-downdraft produced surface perturbations are considerably weaker than both the control simulation and the experiment in which the parameterized moist downdrafts in the Fritsch–Chappell scheme are turned off. Nevertheless, the downdraft produced squall line still survived for more than 9 h in the model and propagated into northeastern Pennsylvania. As will be shown in the next section, the gravity wave played an important role in controlling the propagation of the squall line.

As an aid in understanding the relationship between gravity waves and the evolution of convection, it is helpful to examine how the waves and convection affect the movement of air parcels. Figure 11 shows four representative air trajectories that are obtained (using model-produced hourly wind data) through foreward (1200 to 2100 UTC) and backward (2100 to 1200 UTC) computations of air parcel movement. The parcels originate at various levels and undergo different envi-

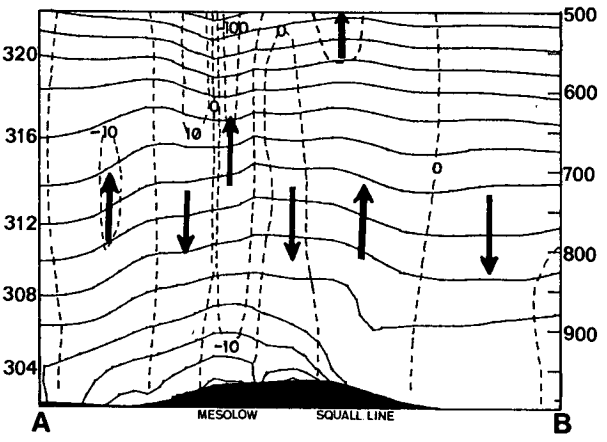

FIG. 10. Vertical cross-section of potential temperature (solid lines, K) and ω (dashed lines, μb s^{-1}). Cross section taken along line AB in 6 h forecast (see Fig. 5a). Large arrows indicate direction of vertical motion.

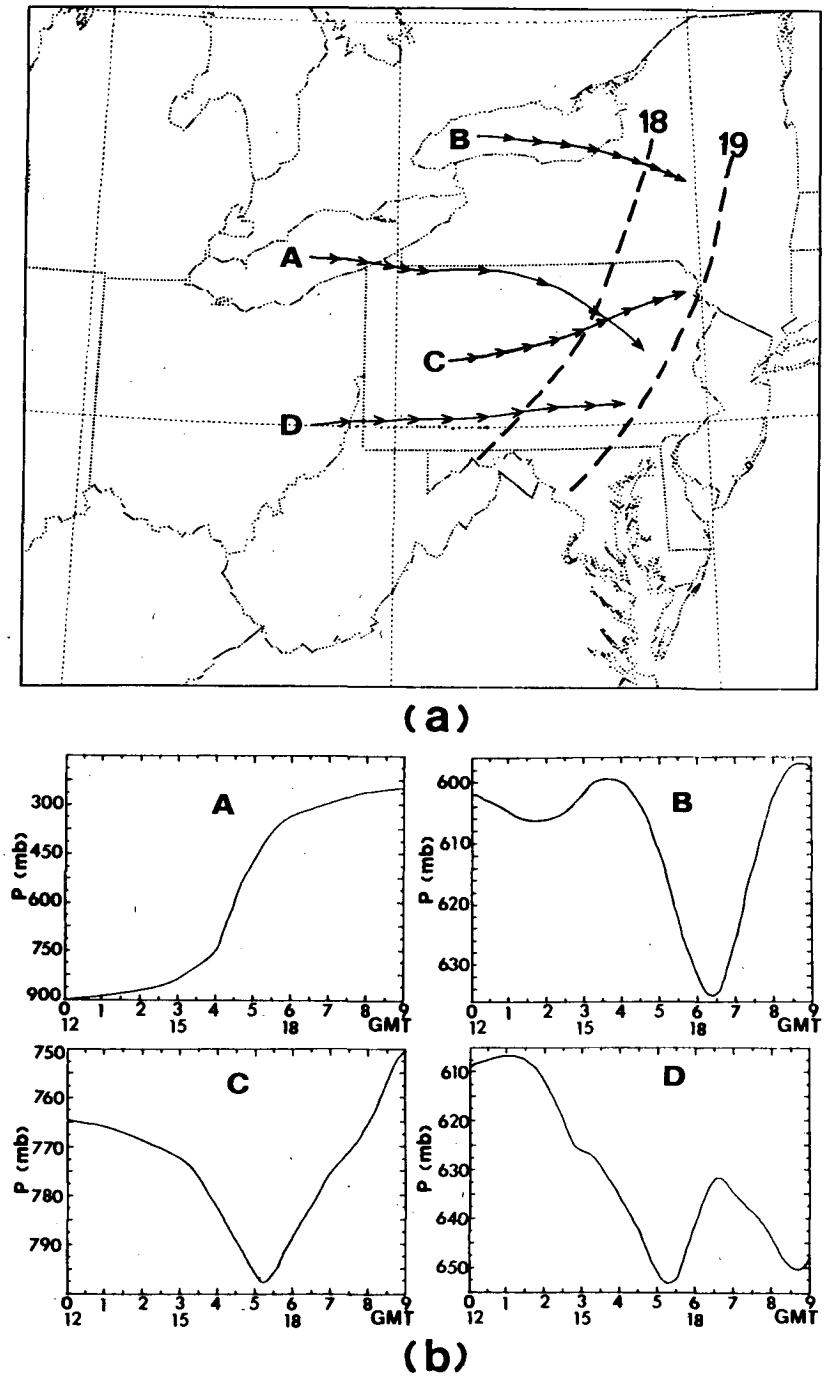

FIG. 11. (a) Horizontal projection of air trajectories between 1200–2100 UTC 19 July 1977. Arrows and their intervals denote the directions and hourly displacement, respectively, of parcel movement. Dashed lines show the location of the simulated pressure trough axis at 1800 and 1900 UTC; (b) Vertical displacement of air parcels as a function of time.

ronments relative to the propagation of the MCSs and waves. The positions of the sea-level pressure troughs at 1800 and 1900 UTC are also displayed. It is evident that air parcels displace much more slowly than gravity waves. All parcels except parcel A exhibit a descending motion as they travel ahead of the pressure trough axis, and then a changeover to an ascending motion occurs as the trailing pressure ridge axis overtakes them. Because these parcels move with and in the same direction as the waves, their oscillation periods are longer than

the wave passage. As can be seen, parcel A originates from the center of the initial convective region at the 900 mb level (where the low-level jet is located). Since the wave perturbation during initial development stage is very weak, little oscillation occurs with this parcel. It appears to be trapped within the mesovortex circulation and, through mesoscale ascent, eventually joins an upper-level anticyclonic outflow. The trajectory of parcel B is basically outside of but still near the area of convective propagation. Interestingly, the gravity wave, with an amplitude of less than 0.6–0.7 mb in the present case, can produce a parcel lifting/lowering of more than 30 mb. Such a vertical displacement is sufficiently large to alternately suppress cloud development and then trigger new convection if the surrounding atmosphere is close to saturation and conditionally unstable. This magnitude of vertical displacement agrees well with a theoretical value computed from a simple Eom-Uccellini formulation, $D = H_1 p'/\rho c^2$ where D is the maximum vertical displacement, H_1 is the height of the midtroposphere in this case, p' is the magnitude of the pressure perturbation, ρ is air density and c is the wave phase velocity. Thus, assuming $H_1 \approx 4500$ m, $p' = 50$ pascal, $\rho = 0.75$ kg m^{-3} and $c \approx 27.5$ m s^{-1} yields $D \approx 400$ m.

As the trajectory of parcel C indicates, when convection can provide further positive forcing, a much larger upward displacement is realized. However, this does not appear to be true for parcel D since convective forcing over southern Pennsylvania was relatively weak and localized. Furthermore, as mentioned before, a pressure tendency ridge propagates ahead of the southern portions of the convection, and tends to produce a negative forcing. This results in a downward displacement of more than 20 mb, thus tending to suppress convective development.

It is important to point out that in the present case there appears to be an absence of a critical level, as noted by numerous theoretical and observational studies (e.g., Lalas and Einaudi, 1976; Lindzen and Tung, 1976; Stobie et al., 1983). The phase speed of the wave propagation is found to be larger than the wind speed at all levels (see Figs. 7–9 in Zhang and Fritsch, 1987), just as in the case described by Uccellini (1975). The absence of a critical level may be partly responsible for the rapid dissipation of the gravity waves as they propagate away from the intense convection.

In addition to the traveling internal gravity waves, quasi-stationary gravity waves associated with the Appalachians occur in the model simulation (see Fig. 12a). It is found that the mountain waves are most apparent at lower levels and at a later integration time than the traveling waves. The mountain waves occur over West Virginia and Maryland, downstream of the highest terrain feature (Fig. 12b). The wavelength of these mountain waves is about 6–8 grid elements. Note that the quasi-stationary divergence/convergence couplet near the southeastern corner of the model domain is not a mountain wave. Rather, it is associated with a sea breeze which results from the large temperature gradient along the land and ocean interface. This will be shown in the next section. These quasi-stationary waves affect the southeastward propagation of the gravity waves associated with the MCSs (cf. Fig. 7), but contribute little to the generation of deep convection during the daytime period because of the much lower-θ_e air present to the east of the Appalachians (see Zhang and Fritsch, 1986a).

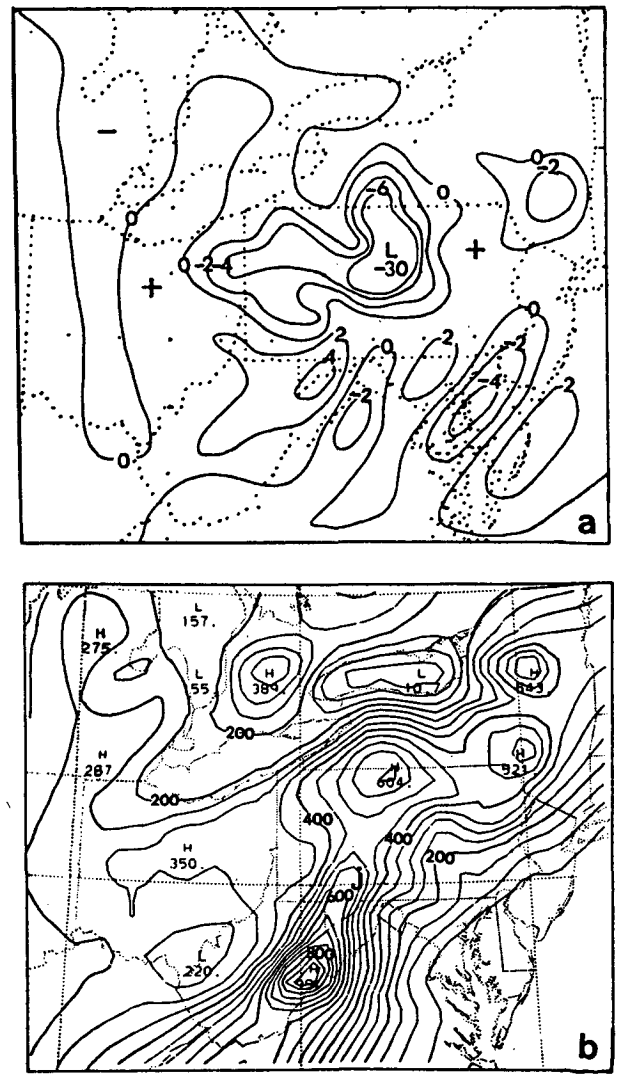

FIG. 12. (a) Simulated 900 mb divergence distribution (10^{-5} s^{-1}) verified at 0000 UTC 20 July, showing the configuration of mountain waves in the model simulation; (b) terrain distribution of the fine mesh.

4. Wave origin and interaction mechanism

As mentioned in the Introduction, the topic of internal gravity waves has not been investigated numer-

ically as often as observationally. Two basic problems in performing real data numerical model case studies are the difficulty in controlling spurious propagation of external gravity waves and the technical difficulty of separating the numerical wave modes from the physically meaningful wave modes. The lack of certain model physics also probably affects the generation of internal gravity waves. As listed in section 1, there are several mechanisms for the interaction between gravity waves and deep convection. The correlation between convective development and wave activity from both observations and numerical simulation suggests that a wave-CISK mechanism may be operating, albeit intermittantly (see Lindzen, 1974; Raymond, 1976; Raymond, 1984; Xu and Clark, 1984). According to the theory, the gravity waves tend to help organize the deep convection while the deep convection tends to enhance or generate gravity waves. This seems to be the case for the organized line structure in the present case. An important question, however, is what mechanism is responsible for the initial generation of the gravity waves? Are they forced by the deep convection? Preexisting sheared flow? Or is it some other mechanism?

To learn more about the wave formation mechanisms and gain further insight into the relationship between the gravity waves and the squall line, several additional experimental simulations have been conducted. Figure 13 shows the sea-level pressure and 850 mb vertical motion fields from an experiment in which the effects of both convective and resolvable-scale heating are excluded (Expt. NDH). Except for the effects of mountainous terrain and variations in surface energy fluxes, the model dynamics are basically determined by the geostrophic adjustment processes. Interestingly, for the same time period examined in the previous parts of this study (1800–2100 UTC), a weak perturbation appears in approximately the same location as the squall line. Moreover, the vertical motion is reasonably well correlated with the sea-level pressure perturbation, i.e., upward motion basically occurs between the trough and advancing pressure ridge, as dictated by the gravity wave theory. There is a downward motion band followed by an upward motion band propagating southeastward in the same manner as the observed and control-simulated squall lines. This indicates that the gravity wave signal may be contained in the initial conditions rather than generated by model convection. Based upon the additional fact that the banded structure in Expt. NDH is most apparent in the lower levels (not shown), it appears that the supergeostrophic low-level jet over the Great Lakes at the initial time is responsible for the generation of the gravity waves through geostrophic adjustment processes. In addition, another experimental simulation, in which the initial winds over the northwestern quadrant of the model domain are substantially weakened (see Zhang and Fritsch, 1986b), shows that the free

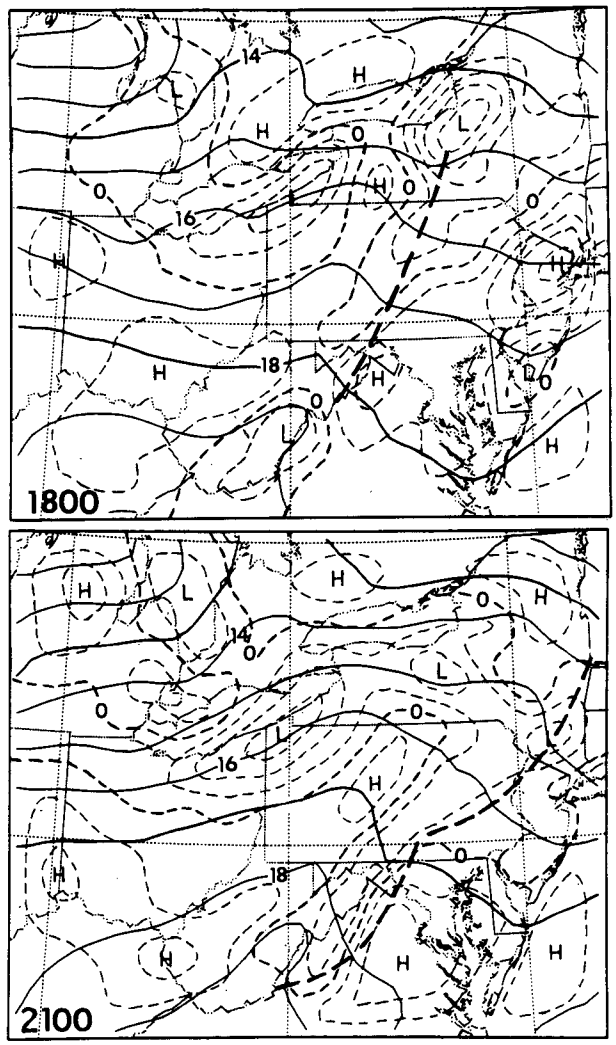

FIG. 13. Simulated 850 mb vertical motion (dashed lines, interval is 1 μb s^{-1}) and sea-level pressure (solid lines, mb) for no diabatic heating run (Expt. NDH). The letters "H" and "L" denote the relative high and low values of vertical motion (ω). The heavy dashed lines denote pressure troughs.

propagating gravity waves are indistinct and poorly organized (not shown). In fact, with this initial condition, the simulated squall line is not nearly as well configured as the control simulation (see Expt. NUV in Zhang and Fritsch, 1986b). It is also interesting to note in Fig. 13 that at 1800 UTC the first wave separates from the original convective region as did the squall line. The upward motion belt over northwestern Pennsylvania is found to be almost stationary until model evening time and is believed to result from the combination of terrain forcing, meso-α scale short-wave forcing, and the temperature contrast between the land and lake water surfaces. To look further into the free wave propagating characteristics, the mountainous terrain in Expt. NDH is replaced by a domain-averaged value of roughly 300 m. The results show that the pressure ridge

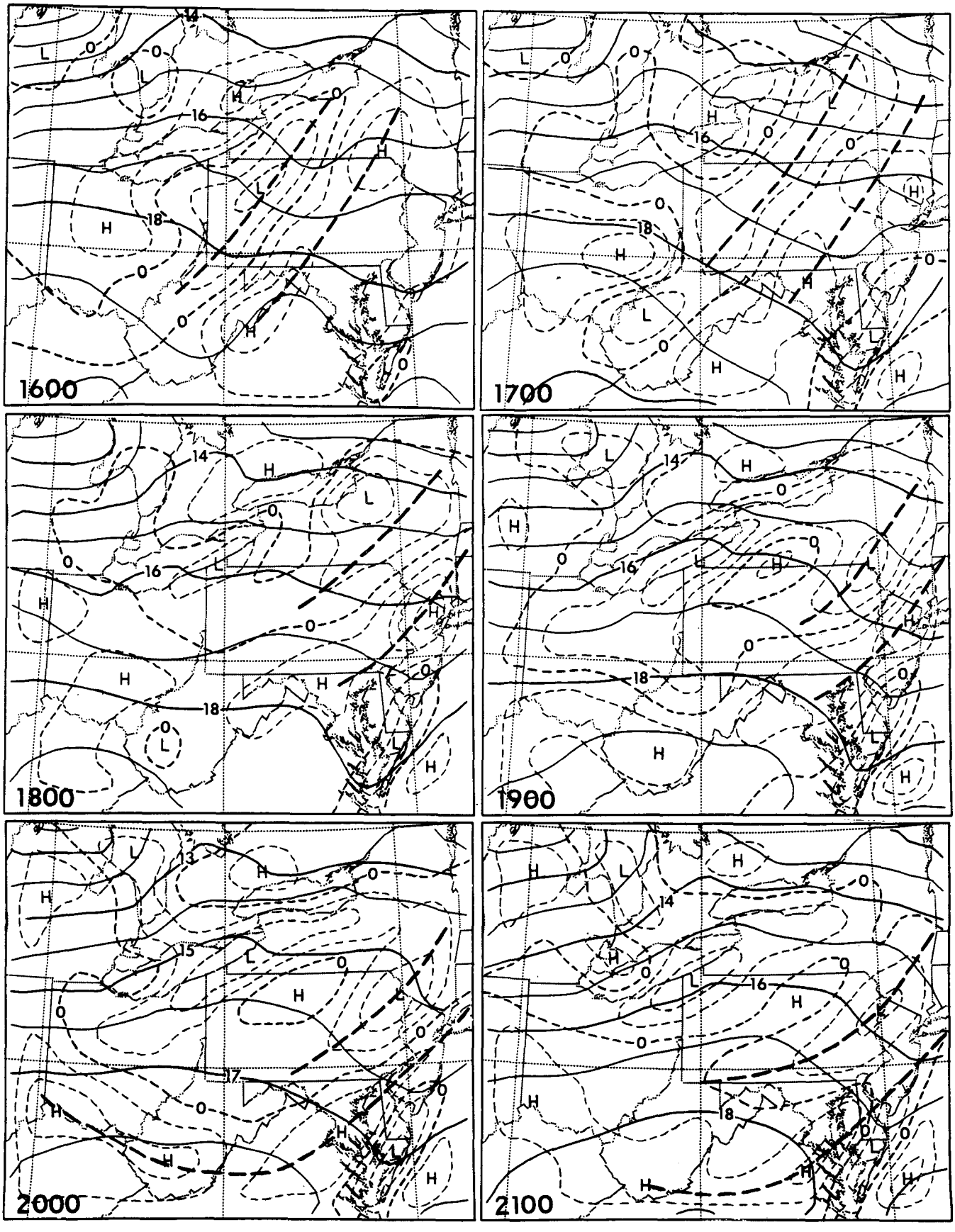

FIG. 14. As in Fig. 13 but for constant terrain and no diabatic heating simulation. The heavy dashed lines denote trough or ridge axis of the 850 mb vertical motion.

associated with the Appalachians is no longer present but the gravity wave propagation becomes more clearly apparent (see Fig. 14). The orientation, wavelength and speed of the wave propagation resemble the control wave characteristics except that the wave strength is weaker. These additional experimental simulations plus the control run suggest that the gravity waves helped the organization and basically determined the evolution of the squall line. Had the environmental conditions been more convectively favorable, the squall line probably would have advanced farther to the east. Since the terrain forcing was eliminated to obtain Fig. 14, it is now possible to recognize that the stationary wave over the southeastern corner of the domain is actually associated with a sea breeze circulation, as mentioned before.

While geostrophic adjustment was responsible for the generation of the first gravity wave, the organized convection helped enhance the gravity waves through thermal forcing and convectively forced "obstacle" effects. This can be seen clearly by comparing the distribution of vertical motion shown in Figs. 8 and 14; the convectively forced wave oscillation is much stronger than the free propagating waves. It is important to point out that the free gravity waves do not seem to help the evolution of the model MCC since the waves propagate in a southwest–northeast orientation while the well-developed MCC exhibits an east–west direction. The physical interactions between the gravity waves and the squall line in the present case can be understood as follows. The atmospheric stratification ahead of the meso-α scale short-wave trough is conditionally unstable. The descending motion produced by the gravity waves tends to temporarily prohibit the occurrence of convective overturning until the approaching positive forcing by the waves and convection can lift an air parcel to saturation. In this regard, the formation mechanism of mesolows or pressure troughs in advance of convective clouds, which was proposed by Hoxit et al. (1976), might be considered a gravity wave phenomenon. Specifically, if environmental conditions are so favorable that the organized convective system can propagate at the same speed as the generated gravity waves, the subsidence warming within a vertical column is capable of producing a strong pressure trough or even closed low ahead of the convective system. The present case study indicates such a possibility. The meso-β scale surface pressure ridge which follows the subsidence-generated trough, then reverses the vertical motion and plays an important role in initiating and enhancing the deep convection. Because there are no low-level inversions or critical levels to trap the waves, the gravity waves in the present case tend to diminish as they move away from the energy source and encounter progressively lower θ_e air.

While the wave-CISK mechanism can provide a positive feedback between the gravity waves and deep convection, this process appears to depend critically on atmospheric stratification, extent of saturation, wind shear, the strength of the wave forcing, time scale of the wave passage, phase relationship between the convection and waves, etc. Only when the time scale required to trigger convection is of the same order of magnitude as that provided by the gravity wave forcing, and when the intense convection propagates in a "locked phase" with the waves, can the convection and waves interact constructively with each other. Otherwise, even though other environmental conditions are favorable, if the time scale to lift an air parcel to saturation is significantly longer than the wave half-period, a negative feedback can occur, as indicated in Figs. 6–8. This might be one of the reasons why scattered convective storms sometimes develop into an organized MCS, sometimes not, or sometimes the MCS dissipates.

5. Summary and concluding remarks

A case study of gravity wave interaction with deep convection associated with the Johnstown MCSs has been presented using available surface observations and a three-dimensional model simulation of the convective events. Both the observed and simulated behaviors of the squall line, perturbations in surface pressure, potential temperature and vertical motion appear to fit the theory of gravity wave propagation. The deep convection typically initiates behind pressure troughs and ahead of or along the axis of the trailing ridges for positive phase velocity. The opposite is true for a negative phase speed. The zero contours of the simulated vertical motion correspond closely to the perturbation trough axis of surface pressure and potential temperature, with descending motion occurring ahead of the troughs and increasing ascending motion towards the approaching ridge axis. Computations of air trajectories show that the gravity wave, with an amplitude of 0.6 to 0.7 mb and a speed 25–30 m s^{-1} in the present case, is capable of generating a vertical displacement of more than 30 mb.

The model simulations indicate that the gravity waves were initiated through geostrophic adjustment processes from a strong wind shear over an area where an explosive convective development had occurred, and then were enhanced by convective forcing. The waves propagated at a speed significantly faster than the forcing from a meso-α scale geostrophic short wave that was partly responsible for the initial convection and later contributed to the development of an MCC. The waves triggered a line of thunderstorms which advanced eastward in a "locked phase" with the waves prior to the line's mature stage. During this period, the waves and convection interacted constructively with each other to maintain the line structure. As the squall line moved into a convectively less unstable environment, the eastward advancement of deep convection

slowed down whereas the gravity waves continued to propagate with little change in speed. Hence, the waves and convection gradually became out of phase, and tended to interact with each other destructively. Because there were no lower-level inversions or critical levels to trap the wave propagation, the gravity waves diminished as they moved away from the energy source region. The mesovortex and MCC seemed to have also produced internal gravity waves. The westward propagation of these waves triggered convection over northern Ohio while the eastward moving waves eventually overtook and altered the evolution of the squall line. Model simulations also showed the presence of quasi-stationary waves associated with the Appalachians and sea breeze circulations. These waves contributed little to the evolution of the MCSs, at least during the daytime period, because of the lower-θ_e air present to the east of the Appalachians.

The present case study suggests that it is important to distinguish gravity wave propagation from the cold outflow material. During the early stage of development when deep convection and gravity waves propagated in a "locked phase," the gravity waves may be a perturbation superimposed on the surface pressure system and difficult to identify. Model results indicate that preserving the internal gravity wave components in the model initial conditions can be important for modeling the detailed structure and evolution of MCSs. In the present case, only vertically integrated mean divergence is removed to reduce noise early in the model integration and divergence/convergence at individual layers is still maintained. The presence of the layered divergence/convergence is found to be instrumental for the initiation and eastward movement of the MCSs and gravity waves over the Great Lakes–Pennsylvania region.

Acknowledgments. This work was supported by NSF Grants ATM-8418995 and ATM-8711014, and USAF Grants AFOSR-83-0064 and AFOSR-88-0050. The authors are very grateful to Drs. J. Molinari and D. J. Raymond for their critical reviews which helped improve the paper, to L. Uccellini, C. Goff, and S. Koch for beneficial discussions, and to J. Singer and D. Corman for skillfully preparing the manuscript. The first author (D.L.Z.) was partly supported through the Advanced Study Program and the Mesoscale and Microscale Meteorology Division of the National Center for Atmospheric Research (NCAR) which is sponsored by the National Science Foundation. The computations were performed on the NCAR CRAY computer.

REFERENCES

Anthes, R. A., E.-Y. Hsie, D. Keyser and Y.-H. Kuo, 1981: Impact of data and initialization procedures on variations of vertical motion and precipitation in mesoscale models. *Proc. IAMAP Symp.*, Hamburg, 245–257, [ESA Sp-165, 8–10, Rue Mario-Nikis, 75738 Paris, 15, France.]

Atkinson, B. W., 1981: *Mesoscale Atmospheric Circulations.* Academic Press, 495 pp.

Balachandran, N. K., 1980: Gravity waves from thunderstorms. *Mon. Wea. Rev.*, **108,** 804–816.

Bosart, L. F., and J. P. Cussens, 1973: Gravity wave phenomena accompanying east coast cyclogenesis. *Mon. Wea. Rev.*, **101,** 446–454.

——, and F. Sanders, 1981: The Johnstown flood of July 1977: A long-lived convective storm. *J. Atmos. Sci.*, **36,** 1616–1642.

——, and ——, 1986: Mesoscale structure in the Megalopolitan snowstorm of 11–12 February 1983. Part III: A large-amplitude gravity wave. *J. Atmos. Sci.*, **43,** 924–939.

Brill, K. F., L. W. Uccellini, R. P. Burkhart, T. T. Warner and R. A. Anthes, 1985: Numerical simulation of a transverse indirect circulation and low-level jet in the exit region of an upper-level jet. *J. Atmos. Sci.*, **42,** 1306–1320.

Christie, D. R., K. J. Muirhead and A. L. Hales, 1978: On solitary waves in the atmosphere. *J. Atmos. Sci.*, **35,** 805–825.

Clark, T. L., T. Hauf and J. P. Kuettner, 1986: Convectively forced internal gravity waves: Results from two dimensional numerical experiments. *Quart. J. Roy. Meteor. Soc.*, **112,** 899–925.

Curry, M. J., and R. C. Murty, 1974: Thunderstorm-generated gravity waves. *J. Atmos. Sci.*, **31,** 1402–1408.

Doviak, R. J., and R.-S. Ge, 1984: An atmospheric solitary gust observed with a doppler radar, a tall tower and a surface network. *J. Atmos. Sci.*, **41,** 2559–2573.

Einaudi, F., 1984: Interactions between gravity waves and convection. *Dynamics of Mesoscale Weather Systems,* J. B. Klemp, Ed., 591 pp.

——, and D. P. Lalas, 1975: Wave induced instability in an atmosphere near saturation. *J. Atmos. Sci.*, **32,** 536–547.

——, W. L. Clark, D. Fua, J. L. Green and T. E. Van Zandt, 1987: Gravity waves and convection in Colorado during July 1983. *J. Atmos. Sci.*, **44,** 1534–1553.

Eom, J., 1975: Analysis of the internal gravity wave occurrence of April 19, 1970 in the Midwest. *Mon. Wea. Rev.*, **103,** 217–226.

Fritsch, J. M., and C. F. Chappell, 1980: Numerical prediction of convectively driven mesoscale pressure systems. Part I: Convective parameterization. *J. Atmos. Sci.*, **37,** 1722–1733.

Gedzelman, S. D., and R. A. Rilling, 1978: Short-period atmospheric gravity waves: a study of their dynamic and synoptic features. *Mon. Wea. Rev.*, **106,** 196–210.

Goff, R. C., 1976: Vertical structure of thunderstorm outflows. *Mon. Wea. Rev.*, **104,** 1429–1440.

Gossard, E. E., and W. H. Hooke, 1975: Waves in the atmosphere. *Developments in the Atmospheric Science, Vol. 2,* Elsevier Scientific, 456 pp.

Hoxit, L. R., C. F. Chappell and J. M. Fritsch, 1976: Formation of mesolows or pressure troughs in advance of cumulonimbus clouds. *Mon. Wea. Rev.*, **104,** 1419–1428.

——, R. A. Maddox, C. F. Chappell, F. L. Zuckerberg, H. M. Mogil, I. Jones, D. R. Greene, R. E. Saffle and R. A. Scofield, 1978: Meteorological analysis of the Johnstown, Pennsylvania flash flood, 19–20 July 1977. NOAA Tech. Rep. ERL 401-APCL43, 71 pp.

Lalas, D. P., and F. Einaudi, 1976: On the characteristics of gravity waves generated by atmospheric shear layers. *J. Atmos. Sci.*, **33,** 1248–1259.

Lindzen, R. S., 1974: Wave-CISK in the tropics. *J. Atmos. Sci.*, **31,** 156–179.

——, and K. K. Tung, 1976: Banded convective activity and ducted gravity waves. *Mon. Wea. Rev.*, **104,** 1602–1617.

Mastrantonia, G., F. Einaudi and D. Fua, 1976: Generation of gravity waves by jet streams in the atmosphere. *J. Atmos. Sci.*, **33,** 1730–1738.

Miller, D. A., and F. Sanders, 1980: Mesoscale conditions for the severe convection of 3 April 1974 in the east-central United States. *J. Atmos. Sci.*, **37,** 1041–1055.

Raymond, D. J., 1976: Wave-CISK and convective mesosystems. *J. Atmos. Sci.*, **33,** 2392–2398.

——, 1983: Wave-CISK in mass flux form. *J. Atmos. Sci.*, **40,** 2561–2572.

——, 1984: A Wave-CISK model of squall line. *J. Atmos. Sci.*, **41,** 1946–1958.

Tepper, M., 1950: A proposed mechanism for squall lines: the pressure jump line. *J. Meteor.*, **7,** 21–29.

——, 1955: On the generation of pressure jump lines by the impulsive addition of momentum to simple current systems. *J. Meteor.*, **12,** 287–297.

Stobie, J. G., F. Einaudi and L. W. Uccellini, 1983: A case study of gravity waves–convective storms interaction: 9 May 1979. *J. Atmos. Sci.*, **40,** 2804–2830.

Uccellini, L. W., 1975: A case study of apparent gravity wave initiation of severe convective storms. *Mon. Wea. Rev.*, **103,** 497–513.

——, and S. E. Koch, 1987: The synoptic setting and possible source mechanisms for mesoscale gravity wave events. *Mon. Wea. Rev.*, **113,** 721–729.

Xu, Q., and J. H. E. Clark, 1984: Wave CISK and mesoscale convective systems. *J. Atmos. Sci.*, **41,** 2089–2107.

Zhang, D.-L., and J. M. Fritsch, 1986a: Numerical simulation of the meso-β scale structure and evolution of the 1977 Johnstown flood. Part I: Model description and verification. *J. Atmos. Sci.*, **43,** 1913–1943.

——, and ——, 1986b: A case study of the sensitivity of numerical simulation of mesoscale convective systems to varying initial conditions. *Mon. Wea. Rev.*, **114,** 2418–2431.

——, and ——, 1987: Numerical simulation of the meso-β scale structure and evolution of the 1977 Johnstown flood. Part II: Inertially stable warm-core vortex and the mesoscale convective complex. *J. Atmos. Sci.*, **44,** 2593–2612.

——, and ——, 1988: Numerical sensitivity experiments of varying model physics on the structure, evolution and dynamics of two mesoscale convective systems. *J. Atmos. Sci.*, **45,** 261–293.

——, H.-R. Chang, N. L. Seaman, T. T. Warner and J. M. Fritsch, 1986: A two-way interactive nesting procedure with variable terrain resolution. *Mon. Wea. Rev.*, **114,** 1330–1339.